

Evaluation and comparison of semi-empirical and numerical methods in predicting wave characteristics in the South Caspian Sea

Zahra Hajebi *, Adel Amouzegar **, Seyed Taghi Omid Naeni ***

ARTICLE INFO

RESEARCH PAPER

Article history:

Received:

July 2024

Accepted:

February 2025

Keywords:

wave prediction,
Mike21-SW Model, semi-empirical method,
wave measurement,
coastal engineering

Abstract:

The prediction of wave parameters based on measured wind parameters plays a crucial role in Coastal and Ocean Engineering. This is particularly important in designing coastal and offshore structures, as there may be limited availability of wave measurement stations. In such cases, wave prediction methods can be used as an alternative to estimate wave characteristics during the design phase of various inshore and offshore structures. This research compares the prediction of wave characteristics between different semi-empirical methods and the MIKE21-SW model. For this aim, the measurements of the wave recorder buoy of the Caspian Oil Company are used for wind data as well as wave characteristics. Statistical indices indicate that the SPM method is the most applicable method than other Semi-empirical methods for predicting the wave characteristics. The error of the semi-empirical method is about twice that of the numerical method. There is more correlation between the obtained and measured data in the numerical method compared to the semi-empirical methods.

1. Introduction

There are many methods to forecast wave parameters based on wind parameters. Although many complex numerical methods have been developed to forecast wave parameters with high accuracy, parametric methods are suitable for early coastal and offshore structures design, with less cost and time.

Also, knowledge of wave parameters is fundamental for maritime activities such as marine transportation, offshore exploration, and coastal development, and parametric wave prediction methods are empirical methods. They are methods for forecasting wave height (H) and period (T) at a specific location, according to wind speed (U), fetch length (F), and duration of the storm (t).

Bishop (1983) predicted the characteristics of waves in Lake Ontario by using three semi-empirical methods, JONSWAP, SMB, and Donelan, and introduced the Donelan method as the most applicable. He used waves with limited wavelength conditions to evaluate and compare these three methods [1]. Kazeminejad et al. (2003) analyzed the characteristics of the waves of the Caspian Sea by comparing the semi-empirical methods of CEM and SPM with buoy wind statistics located in Neka. Their results indicate that the SPM method is more applicable for evaluating the Neka waves [2]. Kazeminejad et al. (2005) compared the characteristics of the waves obtained from the fuzzy inference system and the CEM model with wavelength limitation. The results show that the CEM method overestimates the wave height parameter and forecasts the wave period parameter less than the measured value [3]. Siregar et al. (2020) valid the wave Forecasting with the Sverdrup, Munk, and Bretschneider (SMB) Methods using the Easywave Algorithm. Their result indicates that the accuracy of forecasting using the Easywave algorithm is 89.87% and 78.43% for Hs and Ts, respectively [4]. General Regression Neural Networks were used by Juliani and Adytia (2020) for forecasting wave height based on wind information, in a case study in Jakarta

* MSc student, School of Civil Engineering, faculty of engineering, University of Tehran

Corresponding author, Email: zahrahajebi88.th@gmail.com

** School of Civil Engineering, Faculty of Civil Engineering, Persian Gulf University

*** Associate Professor, School of Civil Engineering, faculty of engineering, University of Tehran

Bay [5]. Asma et al. (2012) used Multiple linear regression (MLR) and artificial neural network (ANN) models to describe the significant wave height off Goa, located on the west Indian coast [6]. Salah (2017) evaluates the prediction of wave parameters by using P-M, SPM, and CEM methods on the South Coast of the Mediterranean Sea. Results show that the P-M method with some modification has more accuracy in the predictions than other methods [7]. A computational tool for predicting wind wave characteristics based on the CEM method is presented by Emrecaan (2022). Based on the results, it can be seen that the best approach is the storm-based user-defined duration approach, and the user-defined duration is related to the location's windy weather. [8]. A hybrid method for predicting multi-step-ahead wind and wave conditions was presented by Wu et al. and The proposed method is evaluated by multi-step-ahead predictions [9]. Choi et al. (2018) developed wind-induced wave prediction using revisited methods. The suggested method is assessed by comparing Donelan, SMB, and CEM methods [10].

Suursaar (2011) calibrated a model for predicting wave heights by using wind-forcing data from Estonian coastal meteorological stations. Results show that the long-term return wave may be impacted by possible inhomogeneities in the older wind data [11]. Kamranzad et al. (2011) predict wave height forecasting in Dayyer (the Persian Gulf) by using an artificial neural network (ANN). The results show that the accuracy of the forecasting increases if only the wind parameters are used as model inputs [12]. Abbasi (2022) investigated the accuracy of the semi-empirical CEM method in predicting the characteristics of wind-induced waves in the Strait of Hormuz (SOH). The results show that the accuracy of the semi-empirical method in predicting the wave characteristics was in close agreement with the measured values and the SMB method is suitable for determining the wave characteristics in this area [13]. Semi-empirical methods usually get more attention to predict the characteristics of waves due to their simplicity and economics. By contrast, numerical models involve more time and money, and it is expected that the accuracy of these models is higher than semi-empirical methods based on consumption cost. It should be noted that there are many similar studies to make time-based predictions using parametric wave prediction methods, but this study aims to evaluate and compare the accuracy of semi-empirical and numerical methods in predicting the characteristics of waves in the South Caspian region. Also, Iran has about 750 kilometers of coastline in the Caspian Sea. Critical ports such as Bandar Anzali, Amirabad, Neka, Nowshahr, and Fereidoun Knar are located there. Lots of finance is considered for developing and constructing marine structures in these ports; as a result, accurate prediction of

the wave characteristics has a vital role in developing ports in this region.

MIKE21-SW is developed by the Danish Institute of Hydraulics. The spectral modulus was calculated based on an unstructured grid. This module calculates the development, depletion, and transmission of waves generated by wind and swell waves in offshore and coastal areas[14]. In 2012, the MIKE 21 SW Model was used to carry out wave hindcast experiments in the Indian Ocean[15].Who? studied the Indian southwest coastal waves with the MIKE21 SW model to understand the influences of artificial structures such as mudflats and bulwarks on coastline alterations[16]. The software FLOW-3D can also be used for modeling wave propagation, as demonstrated by Heidarian et al. in 2022 and by Khoshkenesh et al. in 2021, 2022, and 2024. They utilized this software for wave propagation modeling. Additionally, Bonomelli et al. used the Debra model for this purpose in 2024. Moreover, knowledge of estimating environmental roughness and sediment grain size can be employed for wave propagation, as highlighted by Benetti et al. in 2024.[17-28]

2. Simulation details and method

The Caspian Sea is located between 46.5° to 54° East longitude and 36.5° to 47° North latitude and is the largest land-locked body of water in the world.

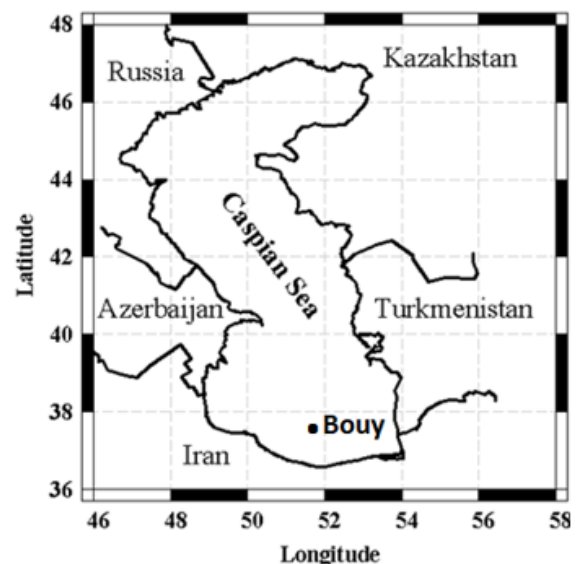


Fig. 1: The location of the wave recorder buoy

2.1. Study area

In this research, the measurements of the wave recorder buoy of the Caspian Oil Company were used for wind data as well as wave characteristics. Khazar Oil Company installed this buoy at a depth of more than 800 meters. As shown in Figure 1, The geographical location of this buoy is 37.8711 degrees North and 51.5137 degrees East. The wind

and wave data recorded with a time step of 1 hour are available for December 2006 to February 2007.

2.2. Numerical simulation

The MIKE21-SW module in the MIKE software package is used to simulate waves.

MIKE21 SW is a spectra-numerical wave forecasting model that provides relatively accurate estimates of wave parameters in coastal areas, seas, and oceans under specific wind, bed, and current conditions. The basis of the methodology used in the MIKE21-SW model is the WAM model, and therefore it has its main capabilities. In the MIKE21 SW model, like most spectral-numerical wave models, even if nonlinear phenomena dominate, the action density spectrum ($N(\sigma, \theta)$) is used to describe the waves instead of the energy density spectrum ($E(\sigma, \theta)$), because the energy density balance is not maintained in the presence of currents. The action density is obtained by dividing the energy density by the relative frequency ($N(\sigma, \theta) = E(\sigma, \theta)/\sigma$). The independent variables are relative frequency (σ) and wave direction (θ) (perpendicular to the wave crest).

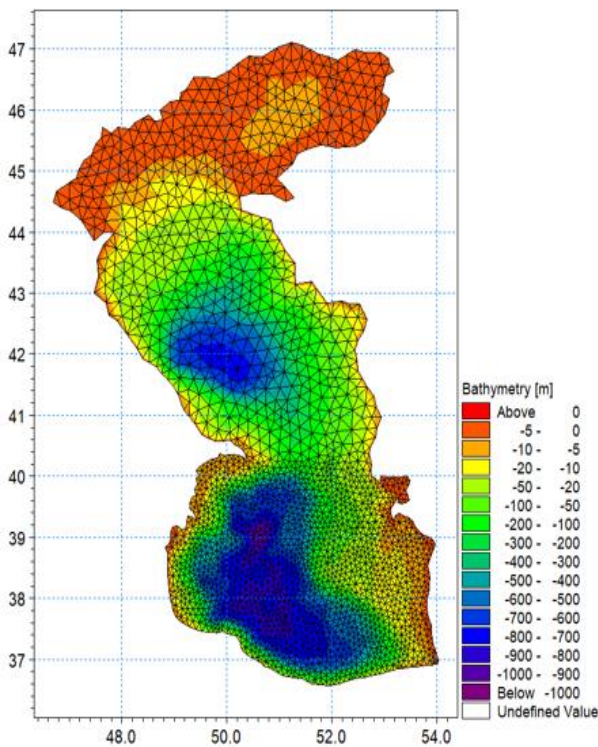


Fig. 2: Gridding and depth measurement file used for numerical simulation with MIKE21-SW model

In the MIKE21 SW model, computational grid files and depth measurement information are given to the model together in one file. The grid used in this model is the triangular grid defiantly. After sensitization, the most optimal size and the number of grids are used. Grid size has

been considered 0.1 to 0.25 degrees in different places. Meshing and depth measurement used for numerical simulation is shown in Figure 2.

The roughness coefficients of the bed and the White capping of the wave have been used to calibrate the model. After calibration, the model is implemented for the current measurement period. Figure 2 compares the height and periodicity of the simulated waves with the measured values at the deep-water buoy location. According to the figure, the values of the height and periodicity of the modeled waves are close to the measured values.

3. Semi-empirical methods

In semi-empirical methods, the height and periodicity of the wave are calculated based on the wind speed, wavelength, and duration of the wind. Based on the existing empirical models, wave growth conditions are usually divided into three conditions: wavelength limitation, wind duration limitation, and fully developed conditions. These methods will be discussed in the following:

3.1. SMB method

In the SMB method, equations (1) calculate wind time duration in limited fetch conditions [29]. Also, equation (2) and Equation (3) are used to calculate the height and periodicity of the wave.

$$t \frac{U}{g} \exp \left[0.8798 \ln \left(\frac{gF}{U^2} \right) + \sqrt{0.0161 \left(\ln \left(\frac{gF}{U^2} \right) \right)^2 - 0.3692 \ln \left(\frac{gF}{U^2} \right) + 2.2024} \right]_{min} \quad (1)$$

In the mentioned equation, t_{min} is the duration time in seconds, U is the wind speed in m/s and F is fetch in meters. Equation (2) and (3) are used to determine the height and periodicity of the wave using the SMB method:

$$H_s = 0.283 \frac{U^2}{g} \tanh \left[0.0125 \left(\frac{gF}{U^2} \right)^{0.42} \right] \quad (2)$$

$$T_s = 1.2 \frac{2\pi U}{g} \tanh \left[0.077 \left(\frac{gF}{U^2} \right)^{0.25} \right] \quad (3)$$

while the actual duration of the wind is smaller than the duration calculated by equation (1), equation (4) is used to determine the effective length of the wave:

$$F = \frac{U^2}{g} \exp \left(\frac{1.76A - 0.369 - \sqrt{0.084A^2 - 1.3A + 6.776}}{1.51} \right) \quad (4)$$

$$A = \ln t - \ln \left(6.59 \frac{U}{g} \right)$$

3.2. SPM method

The empirical wave prediction model using JONSWAP spectra is presented in coastal protection guidelines (SPM,1984) [30]. In the SPM method, equation (5) is used

to calculate the time duration of wind in limited fetch conditions.

$$t_{min} = 68.8 \frac{U_A}{g} \left(\frac{gF}{U_A^2} \right)^{\frac{2}{3}} \quad (5)$$

In the above relation, U_A is the wind stress factor in meters per second and is calculated according to the following equation:

$$U_A = 0.71U^{1.23} \quad (6)$$

If the conditions of wave growth are limited by fetch, the height and periodicity of the waves are calculated from equations (7) and (8).

$$H_{m0} = 0.0016 \frac{U_A^2}{g} \left(\frac{gF}{U_A^2} \right)^{0.5} \quad (7)$$

$$T_P = 0.2857 \frac{U_A}{g} \left(\frac{gF}{U_A^2} \right)^{0.333} \quad (8)$$

Also, the SPM model offers maximum values for the height of the index wave during the periodic period of the peak (spectrum peak). For this purpose, equations (9) and (10) are being used.

$$H_{m0} = 0.2433 \frac{U_A^2}{g} \quad (9)$$

$$T_P = 8.134 \frac{U_A}{g} \quad (10)$$

3.3. CEM method

The CEM method is one of the newest wave forecasting methods presented in the Coastal Engineering Handbook [31]. Based on this method, the minimum duration time on limited fetch is calculated from equation (11). If the actual time duration is greater than t_{min} , the height of the index wave and the peak period could be obtained by equations (12) and (13).

$$t_{min} = 77.23 \frac{F^{0.67}}{U_{10}^{0.34} g^{0.33}} \quad (11)$$

$$H_{m0} = 0.0413 \frac{u_*^2}{g} \left(\frac{gF}{u_*^2} \right)^{0.5} \quad (12)$$

$$T_P = 0.3667 \frac{u_*}{g} \left(\frac{gF}{u_*^2} \right)^{0.333} \quad (13)$$

In the above equations, u_* is the wind shear speed (m/s) calculated from the following relationship:

$$u_* = U_{10} (0.001(1.1 + 0.035U_{10}))^{0.5} \quad (14)$$

Also, the CEM method for calculating the equivalent wavelength in the condition of wind duration limit has given the relation (15), and for the condition of fully developed waves, the relations (16) and (17) have been presented.

Also, equation (15) and equations (16 & 17) are presented for calculating the equivalent fetch for developing and under developing conditions, respectively.

$$X = 0.00523 \frac{u_*^2}{g} \left(\frac{gt}{u_*} \right)^{1.5} \quad (15)$$

$$H_{m0} = 211.5 \frac{u_*^2}{g} \quad (16)$$

$$T_P = 239.8 \frac{u_*}{g} \quad (17)$$

3.4. Bretschneider method

The equation used to obtain the height and periodicity of waves in this method are as follows [32]:

$$F_x = \frac{gF}{U^2}, h_x = \frac{gh}{U^2} \quad (18)$$

$$P_1 = \tanh(0.53h_x^{0.75}), P_2 = \tanh(0.833h_x^{0.375}) \quad (19)$$

$$H_S = 0.283 \frac{U^2}{g} P_1 \tanh \left(\frac{0.0125F_x^{0.42}}{P_1} \right) \quad (20)$$

$$T_P = 7.54 \frac{U}{g} P_2 \tanh \left(\frac{0.077F_x^{0.42}}{P_2} \right) \quad (21)$$

In the above equations, h is the water depth in meters.

3.5. Wilson method

In 1965, Wilson presented an empirical method for predicting waves, and this method is used in predicting waves in the regulations for the design of Japanese ports [33]. Based on this method, the minimum time required for governing fetch limit, t_{min} , is calculated according to the following equation:

$$t_{min} = 43 \frac{F}{U} \left(\frac{gF}{U^2} \right)^{-0.27} \quad (22)$$

If the actual time duration is greater than t_{min} (equation (22)), the wave growth is limited by the fetch length. In this case, the height and periodicity of the index wave can be obtained according to the following equations:

$$H_S = 0.3 \frac{U^2}{g} \left(1 - \left(1 + 0.004 \left(\frac{gF}{U^2} \right)^{0.5} \right)^{-2} \right) \quad (23)$$

$$T_S = 1.37 \frac{2\pi U}{g} \left(1 - \left(1 + 0.008 \left(\frac{gF}{U^2} \right)^{0.33} \right)^{-5} \right) \quad (24)$$

If the actual time duration is smaller than the calculated one by equation (22), the wave growth is limited by the wind duration time. In this case, the equivalent fetch length is calculated by replacing the real duration time in equation (22), and then equations (23) and (24) are calculated.

3.6. Donelan method

Donelan et al. (1985) presented a method for wave conditions with limited fetch by assuming a frequency close to the maximum frequency of the spectrum and that the wind and wave are in the same direction [34]. The following equations are used to obtain the characteristics of the wave:

$$H_S = 0.00366 \frac{U^2}{g} \left(\frac{gF}{U^2} \right)^{0.38} \quad (25)$$

$$T_P = 0.542 \frac{U}{g} \left(\frac{gF}{U^2} \right)^{0.23} \quad (26)$$

4. Results and discussion

The wind measured by the buoy has been used as the input wind of the empirical method and numerical model. The roughness coefficients of the bed and the White capping of the wave have been used to calibrate the numerical model [35-38].

Figure 3 compares the height and periodicity of the simulated waves with the measured values. The height and periodicity of the modeled waves are close to the measured values.

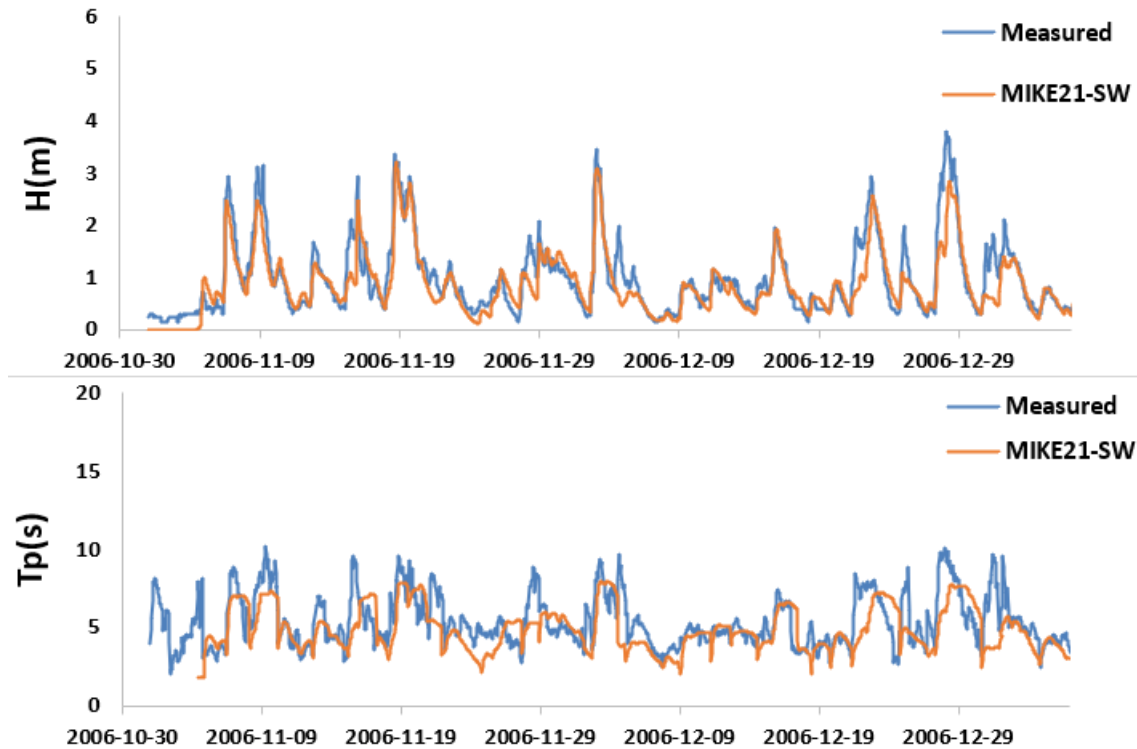


Fig. 3: Comparison of the time series of the height and periodicity of the measured buoy waves and the simulated values using the MIKE21-SW numerical model for November and December 2006

Also, the prediction results of wave characteristics using empirical relationships were evaluated. The comparison of the time series of wave height predicted by different practical methods and measured buoy values is shown in Figure 4 to Figure 9. By comparing these figures, it can be seen that the SPM method provides a better prediction of the height and period values of the measured waves.

To better evaluate these methods, statistical parameters that indicate the accuracy of matching predictions with measurements have been used. These parameters include agreement index (Ia) or efficiency coefficient, dispersion index (SI), correlation coefficient (CC) or (R), bias index (BIAS), and root mean square errors (RMSE), which are defined as follows:

$$ModelSkill = I_a = 1 - \frac{\sum (x_p - x_m)^2}{\sum (|x_p - \bar{x}_m| + |x_m - \bar{x}_m|)^2} \quad (27)$$

$$SI = \frac{\sqrt{\frac{1}{N} \sum_{i=1}^N (x_p - x_m)^2}}{\bar{x}_m} \quad (28)$$

$$CC = R = \frac{\sum (x_p - \bar{x}_p)(x_m - \bar{x}_m)}{\sqrt{\sum (x_p - \bar{x}_p)^2 \sum (x_m - \bar{x}_m)^2}} \quad (29)$$

$$BIAS = \sum \frac{1}{N} (X_p - X_m) \quad (30)$$

$$RMSE = \sqrt{\frac{1}{N} \sum (X_p - X_m)^2} \quad (31)$$

In the number of data, the predicted value, and the measured value and the average of the measured and predicted data, respectively. The results of the calculation of these parameters for different wave forecasting methods and the height and periodicity of the waves are presented in Table 1 and Table 2, respectively. As can be seen, based on the skewness index, all the methods used underestimated the height and period of the wave. In addition, all the methods have predicted the peak period with a greater error than the height of the index wave. By comparing the statistical parameters of different methods, it can be seen that the SPM method is somewhat more accurate than other methods in predicting the height and peak period of the wave. It should

be noted that the obtained results are consistent with the results of other researchers [3]. According to Tables 1 and 2, as can be seen, the values simulated using the MIKE21-SW numerical model compared to the experimental methods, the accuracy of the

numerical simulation is much higher than the semi-empirical methods. The error of these methods in predicting the wave height is about twice the error of the numerical method (based on SI and RMSE indices).

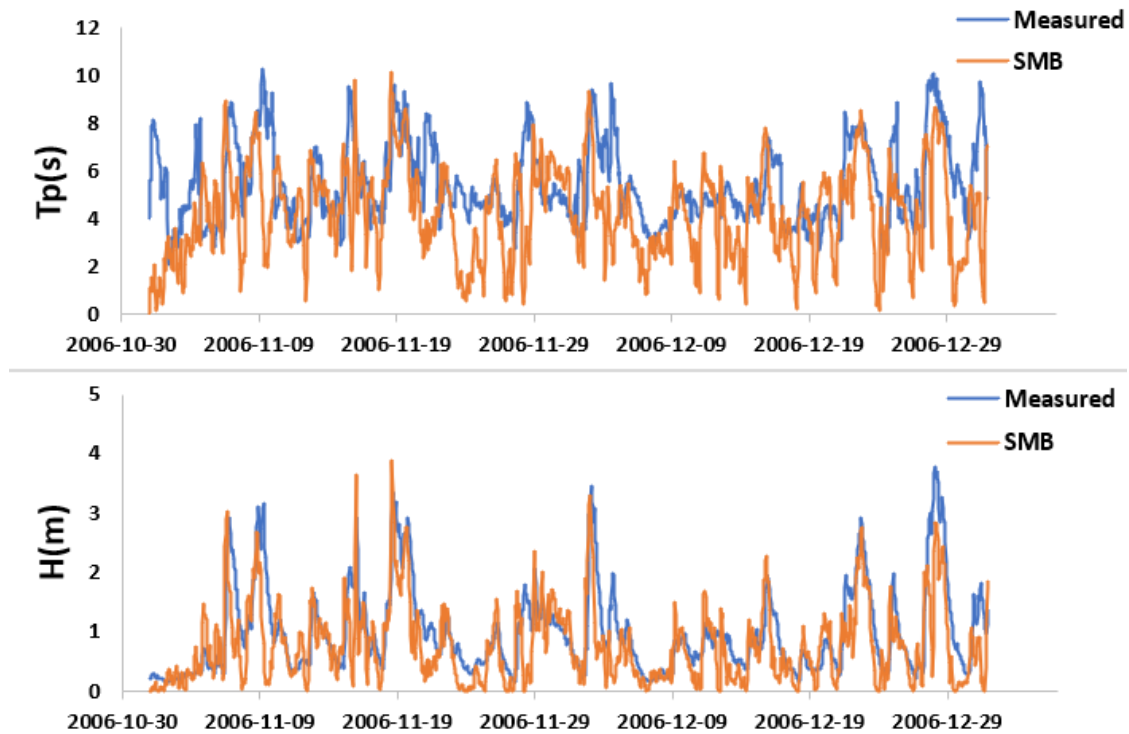


Fig. 4: Comparison of the time series of the height And periodicity of the measured buoy waves and the values predicted by the SMB experimental method for November and December 2006

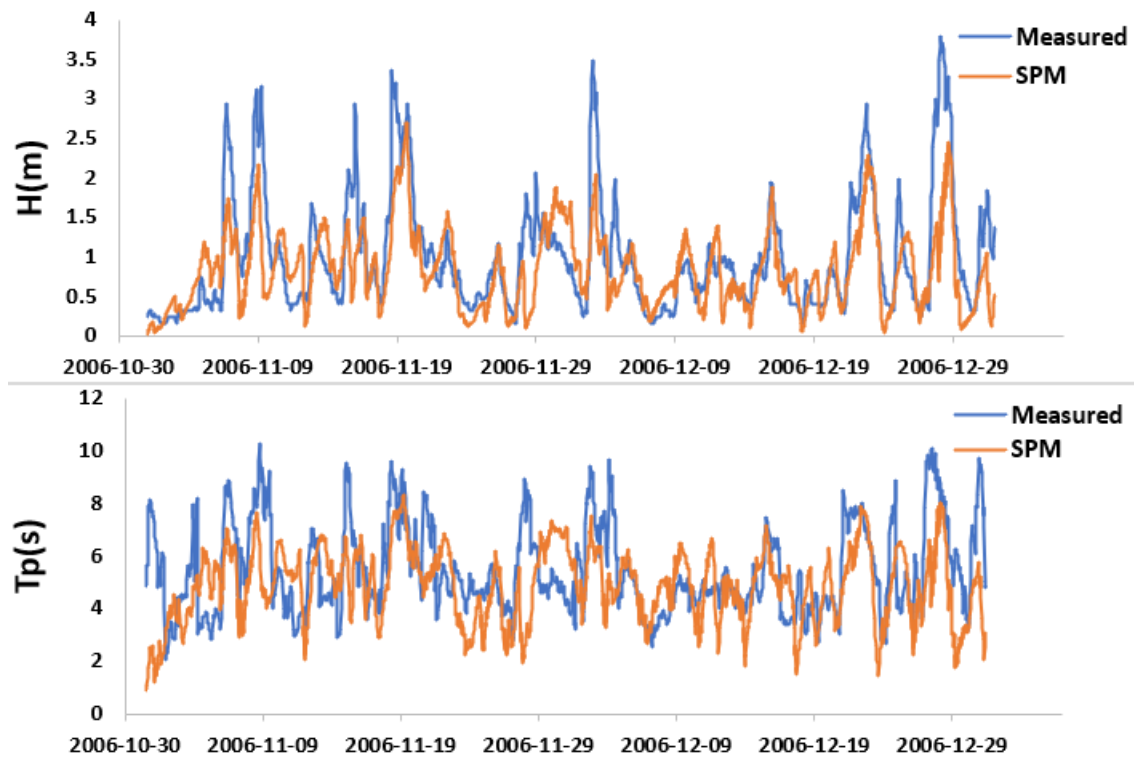


Fig. 5: Comparison of the time series of the height And periodicity of the measured buoy waves and the values predicted by the SPM experimental method for November and December 2006

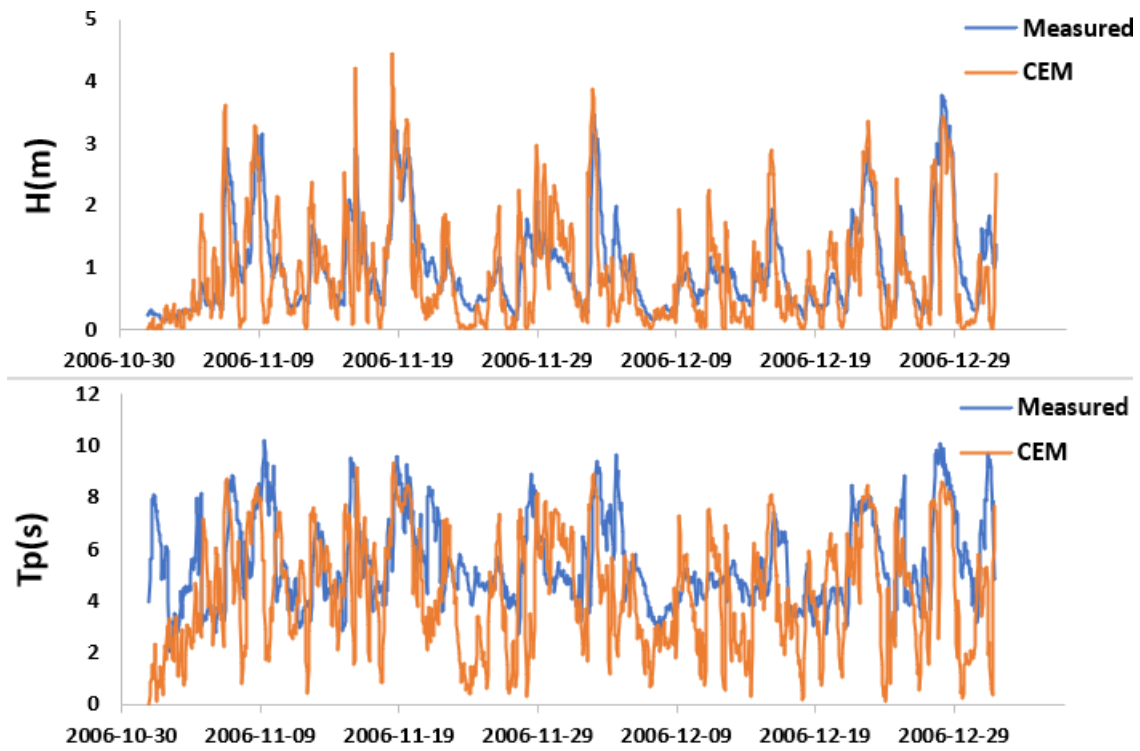


Fig. 6: Comparison of the time series of the height and periodicity of the measured buoy waves and the values predicted by the experimental CEM method for November and December 2006

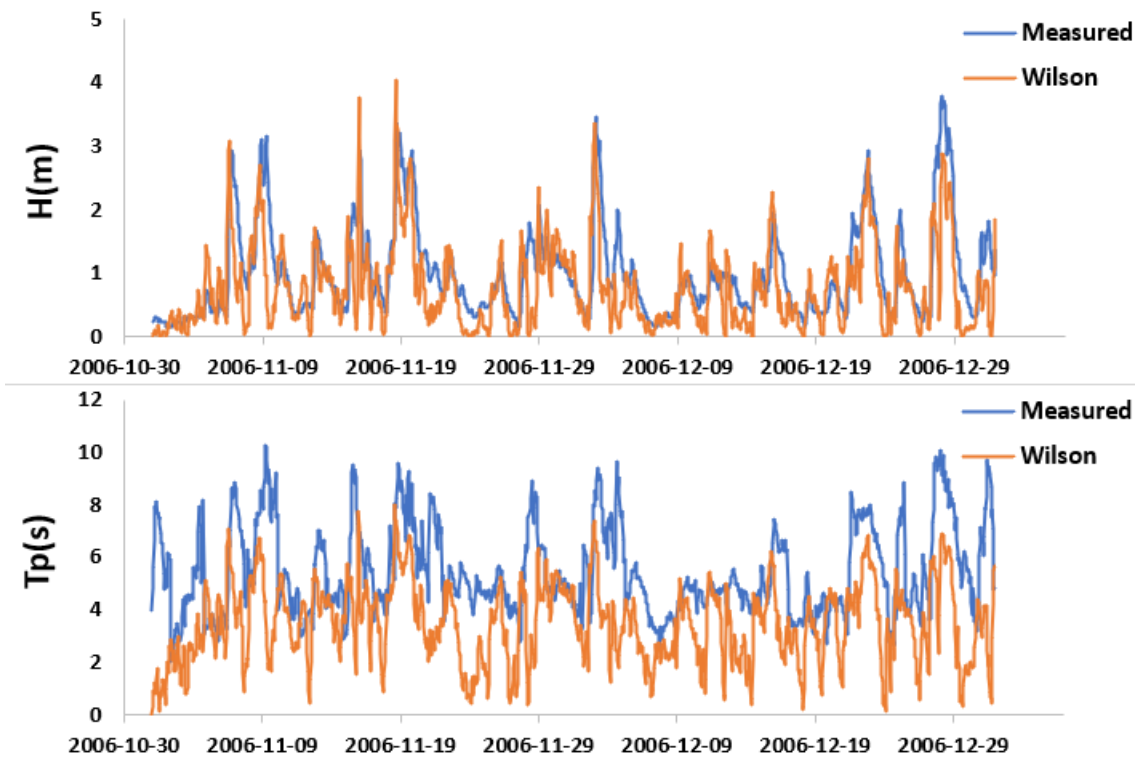


Fig. 7: Comparison of the time series of the height and periodicity of the measured buoy waves and the values predicted by Bretschneider's experimental method for November and December 2006

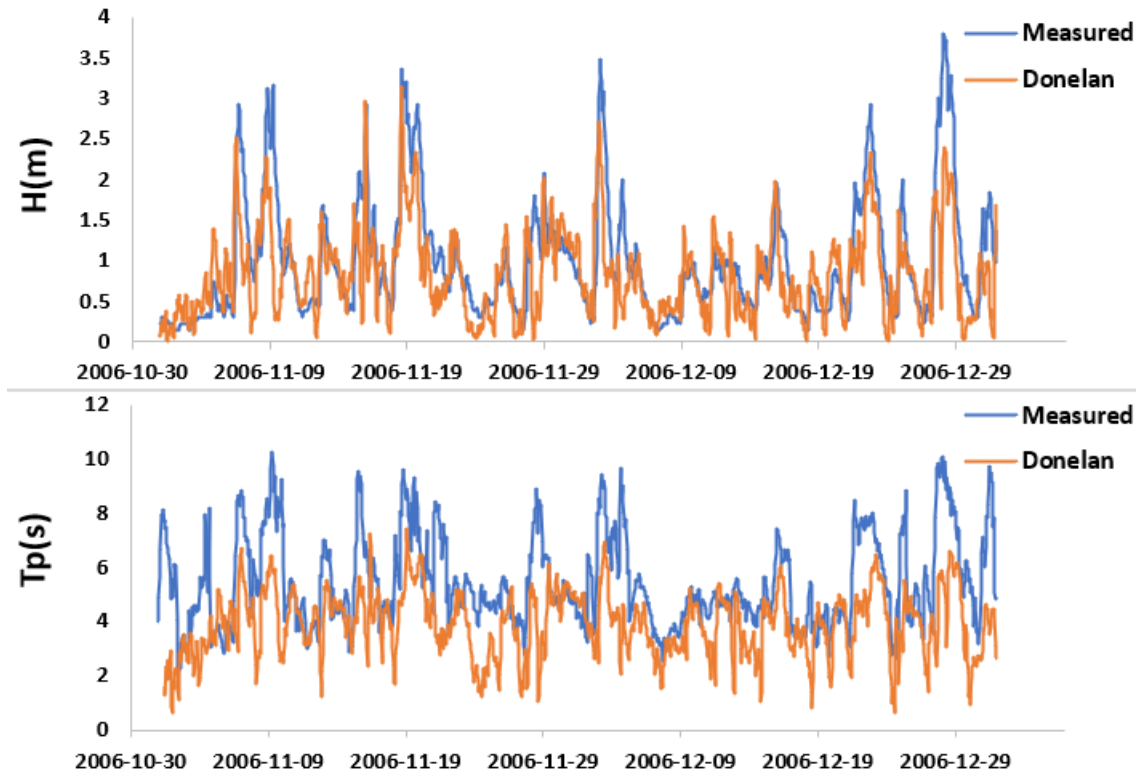


Fig. 8: Comparison of the time series of the height and periodicity of the measured buoy waves and the values predicted by Wilson's experimental method for November and December 2006

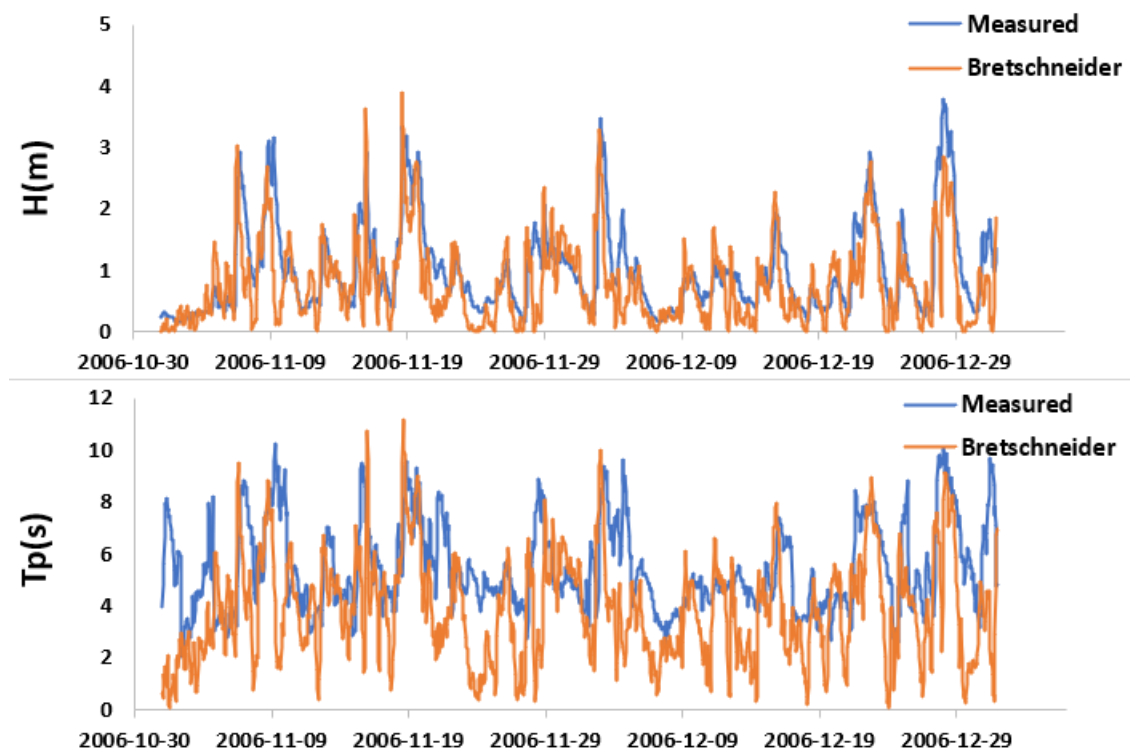


Fig. 9: Comparison of the time series of the height and periodicity of the measured buoy waves and the values predicted by Donelan's experimental method for November and December 2006

Table 1: Error indices for different wave forecasting methods and wave height values

	SEM	SPM	CEM	Bretschneider	Wilson	Donelan	MIKE21-SW
<i>Ia</i>	0.17	0.17	0.17	0.17	0.17	0.20	0.08
<i>SI</i>	0.56	0.51	0.57	0.56	0.57	0.54	0.35
<i>CC or R</i>	0.73	0.74	0.73	0.72	0.73	0.71	0.88
<i>BIAS</i>	-0.22	-0.04	-0.24	-0.22	-0.24	-0.17	-0.11
<i>RMSE</i>	0.57	0.52	0.57	0.57	0.57	0.55	0.36

Table 2: Error indices for different wave forecasting methods and wave period values

	SMB	SPM	CEM	Bretschneider	Wilson	Donelan	MIKE21-SW
<i>Ia</i>	0.42	0.42	0.42	0.44	0.48	0.47	0.28
<i>SI</i>	0.43	0.40	0.46	0.48	0.49	0.42	0.29
<i>CC or R</i>	0.36	0.37	0.34	0.37	0.36	0.35	0.55
<i>BIAS</i>	-1.13	-0.95	-1.04	-1.52	-1.91	-1.49	-0.51
<i>RMSE</i>	2.34	2.12	2.48	2.59	2.64	2.26	1.57

In the ISWM project [39], based on various authoritative sources, the typical values of each of the above parameters for evaluating wave height values were presented in Table 3. Therefore, the value of error indicators for wave height can be evaluated using the values in this table. Comparing the results of the error indices presented in Table 1 and the permissible values given in Table 3 shows that all the error indices are in the ideal range for numerical simulation and the normal range for experimental methods. Therefore, the accuracy of predictions of both suitable techniques and numerical simulation is perfect.

Table 3: Usual and permissible values of different statistical parameters for wave height prediction

parameter	unit	Normal range	Ideal range
<i>Ia</i>	-	0.7 – 0.95	> 0.8
<i>SI</i>	percent	0.15 – 0.35	< 0.35
<i>CC</i>	-	0.75 – 0.90	> 0.8
<i>BIAS</i>	m	0.2 – 0.5	< 0.3
<i>RMSE</i>	m	0.1 – 0.7	< 0.5

5. Conclusions

In this research, the accuracy of semi-empirical and numerical methods in predicting the characteristics of wind waves in the South Caspian deep water region has been studied, evaluated, and compared. The characteristics of the waves have been calculated using more than 4350 wind data collected in the wave recorder buoy located in the deep-water area and using different semi-empirical methods.

After that, the values of the height and period of the predicted waves were compared with the characteristics recorded by the wave recorder buoy, and the errors of the semi-empirical methods were determined. Then, numerical simulation was conducted using wind buoy data and the SW model of MIKE21 software, and the results of this model were compared with the results of semi-empirical methods. The important findings can be summarized as follows:

- Based on the BIAS index, Semi-empirical methods predict the average wave height and periodicity less than the actual value.
- Overall, Statistical indexes indicate that the SPM method is the most applicable method for predicting the wave heights and periods
- The calculated statistical indicators, except the RMSE index, show that semi-empirical methods can predict the heights more accurately than the periods.
- Based on statistical indicators, the results of comparing semi-empirical and numerical methods show that the error of the semi-empirical method in predicting the characteristics of waves is about twice of the numerical method. In contrast, numerical methods were recommended for predicting wave characteristics. This should be investigated in future studies.

6. References

- [1] Bishop, C. T. (1983). Comparison of manual wave prediction models. *Journal of Waterway, Port, Coastal, and Ocean Engineering*, 109(1), 1-17.
- [2] Kazeminezhad, M.H., Etemad-Shahidi, A., Mousavi, S.J. (2004), "Application of Simplified Methods in the Prediction of Wave Parameters in Neka", 6th International Conference on Coastal, Ports & Marine Structures.

- [3] Kazeminezhad, M.H, Etemad-Shahidi, A., Mousavi, S.J. (2005), "Application of Fuzzy Inference System in the Prediction of Wave Parameters", *J. Ocean Engineering*, 32 (2005) pp 1709–1725.
- [4] Siregar, G. R. S., Alfarizi, H., Purnomo, F. M., Ginanjar, S., & Wirasatriya, A. (2020). Validation of Wave Forecasting with the Sverdrup, Munk, and Bretschneider (SMB) Method Using Easywave Algorithm. In 2020 IEEE Asia-Pacific Conference on Geoscience, Electronics and Remote Sensing Technology (AGERS) (pp. 11-15). IEEE.
- [5] Juliani, V., & Adytia, D. (2020). Wave Height Prediction based on Wind Information by using General Regression Neural Network, study case in Jakarta Bay. In 2020 8th International Conference on Information and Communication Technology (ICoICT) (pp. 1-5). IEEE.
- [6] Asma, S., Sezer, A., & Ozdemir, O. (2012). MLR and ANN models of significant wave height on the west coast of India. *Computers & Geosciences*, 49, 231-237.
- [7] Salah, H. (2017). Evaluate the Prediction of Wave Parameters Using Parametric Methods in the South Coast of the Mediterranean Sea.
- [8] Emrecan, P. (2022). A computational tool for wind wave prediction based on CEM method (Master's thesis, Middle East Technical University).
- [9] Wu, M., Stefanakos, C., Gao, Z., & Haver, S. (2019). Prediction of short-term wind and wave conditions for marine operations using a multi-step-ahead decomposition-ANFIS model and quantification of its uncertainty. *Ocean Engineering*, 188, 106300.
- [10] Choi, B. Y., Jo, H. J., Lee, K. H., & Byoun, D. H. (2018). Development of Wind Induced Wave Predict Using Revisited Methods. *Journal of Advanced Research in Ocean Engineering*, 4(3), 124-134.
- [11] Suursaar, Ü. (2013). Locally calibrated wave hindcasts in the Estonian coastal sea in 1966-2011. *Estonian Journal of Earth Sciences*, 62(1), 42.
- [12] Kamranzad, B., Etemad-Shahidi, A., & Kazeminezhad, M. H. (2011). Wave height forecasting in Dayyer, the Persian Gulf. *Ocean engineering*, 38(1), 248-255.
- [13] abbasi, M. R. (2019). Evaluating semi-empirical wave forecasting method CEM in the Strait of Hormuz. *International Journal of Coastal and Offshore Engineering*, 3(3), 43–46.
- [14] DHI, 2016. MIKE11, MIKE21FM, MIKESW, User Manual.
- [15] Remya, P. G., Kumar, R., Basu, S., & Sarkar, A. (2012). Wave hindcast experiments in the Indian Ocean using MIKE 21 SW model. *Journal of earth system science*, 121, 385-392.
- [16] Noujas, V., Thomas, K. V., & Ajeesh, N. R. (2017). Shoreline management plan for a protected but eroding coast along the southwest coast of India. *International Journal of Sediment Research*, 32(4), 495-505.
- [17] Heidarian, P., Neyshabouri, S. A. A. S., Khoshkonesh, A., Bahmanpouri, F., Nsom, B., & Eidi, A. (2022). Numerical study of flow characteristics and energy dissipation over the slotted roller bucket system. *Modeling Earth Systems and Environment*, 8(4), 5337–5351. <https://doi.org/10.1007/s40808-022-01372-z>
- [18] Khoshkonesh, A., Nsom, B., Okhravi, S., Ahmadi Dehrashid, F., Heidarian, P., & DiFrancesco, S. (2024). Numerical investigation of dam break flow over erodible beds with diverse substrate level variations. *Journal of Hydrology and Hydromechanics*, 72(1), March 2024. <https://doi.org/10.2478/johh-2023-0040>
- [19] Khoshkonesh, A., Nsom, B., Dehrashid, F. A., Heidarian, P., & Riaz, K. (2021, January). Comparison of the SWE and 3D models in simulation of the dam-break flow over the mobile bed. In Fifth scientific Conference of applied research in science and technology of Iran.
- [20] Khoshkonesh, A., Asim, T., Mishra, R., Dehrashid, F. A., Heidarian, P., & Nsom, B. (2022). Study the effect of obstacle arrangements on the dam-break flow. *International Journal of COMADEM*, 25(1), 41-50. <https://apscience.org/comadem/index.php/comadem/article/view/301>
- [21] Bonomelli, R., Pilotti, M., & Heidarian, P. (2024). DEBRA: A multi-rheological 2D steep shallow water finite volume scheme for debris flow propagation in mountain areas. EGU General Assembly 2024, Vienna, Austria, 14–19 April 2024. <https://doi.org/10.5194/egusphere-egu24-4141>
- [22] Benetti, M., Heidarian, P., Bonomelli, R., & Pilotti, M. (2024). Exploring remote sensing methodologies for river bed grain size: Insights from a mountainous watershed study in Val Camonica, Italy. EGU General Assembly 2024, Vienna, Austria, 14–19 April 2024. <https://doi.org/10.5194/egusphere-egu24-5752>
- [23] Khoshkonesh, A., Dehrashid, F. A., Nsom, B., Gohari, S., Banejad, H., Heidarian, P. (2021). Dam-break flow regime over mobile beds, a numerical CFD approach. Seminar: INTERNATIONAL CONFERENCE ON SUSTAINABLE DEVELOPMENT AND URBAN CONSTRUCTION. <https://www.sid.ir/paper/949571/en>
- [24] Khoshkonesh, A., Dehrashid, F. A., Nsom, B., Gohari, S., Banejad, H., Heidarian, P. (2021). Dam-break induced flow over mobile beds, numerical approach in volume of fluid method. Seminar: INTERNATIONAL CONFERENCE ON SUSTAINABLE DEVELOPMENT AND URBAN CONSTRUCTION. <https://www.sid.ir/paper/949571/en>
- [25] Khoshkonesh, A., Dehrashid, F. A., Nsom, B., Gohari, S., Banejad, H., Heidarian, P. (2021). Generation the hydraulic jumps by the dam-break flow over the movable beds. Seminar:

INTERNATIONAL CONFERENCE ON SUSTAINABLE DEVELOPMENT AND URBAN CONSTRUCTION. <https://www.sid.ir/paper/949571/en>

[26] Zarrin, Z., Khajavigodellou, Y., & Zoej, M. J. V. (2024). Detection of Land Use Changes in Forests Using Satellite Image Classification Based on Deep Learning: A Case Study of Sardasht Forests. *Journal of Geography, Environment and Earth Science International*, 28(5), 43-51. <https://doi.org/10.9734/jgeesi/2024/v28i5769>

[27] Khajavigodellou, Y., Qi, J., Chen, J., Nejadhashemi, A. P., Moore, N. J., & Zarrin, Z. (2023). Reframing the WEF Nexus to Prevent WEF Bankruptcy: Transboundary River Basin Water-Energy-Food Bankruptcy Challenges and Potential Solutions. *AGU23*.

[28] Khajavigodellou, Y., Qi, J., Chen, J., Moore, N. J., Nejadhashemi, A. P., & Zarrin, Z. (2023). Transboundary Water Resource Conflicts: A New Cold War?. *AGU23*.

[29] Shore Protection Manual" (1984), U.S. Army Coastal Engineer Waterways Station, Vicksburg, MS, 2 Volumes, 4th Edition.

[30] "Shore Protection Manual" (1977), U.S. Army Coastal Engineering Research Center, Fort Belvoir, VA, 3 Volumes, 3rd Edition.

[31] Coastal Engineering Manual" (2003), Chapter II-2: "Meteorology and Wave Climate", Engineer Manual 1110-2-1100, U.S. Army Corps of Engineers, Washington, DC.

[32] Shore Protection Manual or Lecture Notes Holthuijsen (Ocean Wave Theory, P16-19) Calculation acc. To Bretschneider; see SPM or Lecture Notes of Holthuijsen.

[33] Wilson, B.W., 1965. Numerical prediction of ocean waves in the North Atlantic for December 1959. *Deutsche Hydrogen. Z.*, 18(3):114–30.

[34] U.S. Army Coastal Engineering Research Center, Shore Protection Manual, 4th Edition, U.S, Government Printing Office, Washington DC, 120-130, 1984.

[35] Souri, J., OmidvarMohammadi, H., Neyshabouri, S.A.A.S., Chooplou, A.C, Kahrizi, E, & Akbari, H. (2024). Numerical simulation of aeration impact on the performance of a-type rectangular and trapezoidal piano key weirs. *Modeling Earth Systems and Environment*. <https://doi.org/10.1007/s40808-024-02058-4>

[36] Kahrizi, E. (2024). Application of the Image Processing Method and the Beer-Lambert Law for Assessing Sea Water Intrusion in Rivers. *EarthArXiv*. <https://doi.org/10.31223/X50D8K>

[37] Motaei, S., Ghazavi, M., & Rezazadeh, G. (2024). Incorporating temperature-dependent properties into the modeling of photo-thermo-mechanical interactions in cancer tissues. *Thermal Science and Engineering Progress*, 47, 102351. <https://doi.org/10.1016/j.tsep.2023.102351>

[38] Kahrizi, E., Salehi Neyshabouri, S. A. A., Zeynolabedin, A., Souri, J., & Akbari, H. (2023). Experimental evaluation of two-layer air bubble curtains to prevent seawater intrusion into rivers. *Journal of Water and Climate Change*, 14(2), 543–558. <https://doi.org/10.2166/wcc.2023.384>

[39] Golshani, A., Taebi, S., & Chegini, V. (2007). Wave hindcast and extreme value analysis for the southern part of the Caspian Sea. *Coastal engineering journal*, 49(04), 443-459.



This article is an open-access article distributed under the terms and conditions of the Creative Commons Attribution (CC-BY) license.